

# Lawrence Berkeley National Laboratory

## LBL Publications

### Title

Quantifying the energy impact of heat mitigation technologies at the urban scale

### Permalink

<https://escholarship.org/uc/item/3nx8r4ts>

### Journal

Nature Cities, 1(1)

### ISSN

2731-9997

### Authors

Haddad, Shamila

Zhang, Wannu

Paolini, Riccardo

et al.

### Publication Date

2024

### DOI

10.1038/s44284-023-00005-5

### Copyright Information

This work is made available under the terms of a Creative Commons Attribution-NonCommercial License, available at <https://creativecommons.org/licenses/by-nc/4.0/>

Peer reviewed



Building Technologies & Urban Systems Division  
Energy Technologies Area  
Lawrence Berkeley National Laboratory

# Quantifying the energy impact of heat mitigation technologies at the urban scale

Shamila Haddad, Wannu Zhang, Riccardo Paolini, Kai Gao, Muzahim Altheeb, Abdulrahman Al Mogirah, Abdullatif BinMoammar, Tianzhen Hong, Ansar Khan, C. Cartalis, A. Polydorose and Mattheos Santamouris

<sup>1</sup>School of Built Environment, Faculty of Arts, Design and Architecture, University of New South Wales, Sydney, New South Wales, Australia, <sup>2</sup>Building Technology and Urban Systems Division, Lawrence Berkeley National Laboratory, Berkeley, CA, USA, <sup>3</sup>Royal Commission of Riyadh City, Riyadh, Saudi Arabia, <sup>4</sup>Department of Geography, Lalbaba College, University of Calcutta, Kolkata, India, <sup>5</sup>Physics Department, University of Athens, Greece, <sup>6</sup>Anita Lawrence Chair in High Performance Architecture, University of New South Wales, Sydney, New South Wales, Australia

Energy Technologies Area  
January 2024

[doi.org/10.1038/s44284-023-00005-5](https://doi.org/10.1038/s44284-023-00005-5)



This work was supported by the Assistant Secretary for Energy Efficiency and Renewable Energy, Building Technologies Office, of the US Department of Energy under Contract No. DE-AC02-05CH11231.

Disclaimer:

This document was prepared as an account of work sponsored by the United States Government. While this document is believed to contain correct information, neither the United States Government nor any agency thereof, nor the Regents of the University of California, nor any of their employees, makes any warranty, express or implied, or assumes any legal responsibility for the accuracy, completeness, or usefulness of any information, apparatus, product, or process disclosed, or represents that its use would not infringe privately owned rights. Reference herein to any specific commercial product, process, or service by its trade name, trademark, manufacturer, or otherwise, does not necessarily constitute or imply its endorsement, recommendation, or favoring by the United States Government or any agency thereof, or the Regents of the University of California. The views and opinions of authors expressed herein do not necessarily state or reflect those of the United States Government or any agency thereof or the Regents of the University of California.

# Quantifying the energy impact of heat mitigation technologies at the urban scale

Received: 11 September 2023

Accepted: 16 November 2023

Published online: 11 January 2024

 Check for updates

Shamila Haddad<sup>1,7</sup>, Wanni Zhang<sup>2</sup>, Riccardo Paolini<sup>1</sup>, Kai Gao<sup>1,8</sup>,  
Muzahim Altheeb<sup>3</sup>, Abdulrahman Al Mogirah<sup>3</sup>, Abdullatif Bin Moammar<sup>3</sup>,  
Tianzhen Hong<sup>2</sup>, Ansar Khan<sup>4</sup>, Constantinos Cartalis<sup>5</sup>, Anastasios Polydoros<sup>5</sup>  
& Mattheos Santamouris<sup>1,6</sup>  

Advanced urban heat mitigation technologies that involve the use of super-cool materials combined with properly designed green infrastructure lower urban ambient and land surface temperatures and reduce cooling consumption at the city scale. Here we present the results of a large-scale heat mitigation project in Riyadh, Saudi Arabia. Daytime radiative coolers, as well as cool materials combined with irrigated or non-irrigated greenery, were used to design eight holistic heat mitigation scenarios. We assess the climatic impact of the scenarios as well as the corresponding energy benefits of 3,323 urban buildings. An impressive decrease of the peak ambient temperature of up to 4.5 °C is calculated, the highest reported urban ambient temperature reduction, and the annual sum of the differences in the ambient temperature against a standard temperature base (cooling degree hours) in the city decreases by up to 26%. We find that innovative urban heat mitigation strategies contribute to the remarkable cooling energy conservation by up to 16%, and the combined implementation of heat mitigation and energy adaptation technologies decreases the cooling demand by up to 35%.

Cities are one of the largest consumers of energy and emitters of greenhouse gases in the world<sup>1</sup>, so urban areas offer great potential for improvements in energy efficiency and the reduction of greenhouse gases<sup>2</sup>. Cities exhibit higher temperatures than the surrounding areas because of their positive thermal balance<sup>3</sup>. Global climate change is synergistically affecting urban temperatures, increasing the magnitude of overheating<sup>4,5</sup>. About 13,000 cities are exhibiting overheating problems, measured as up to 10.0 °C, and more than 1.7 billion people are living under severe overheating conditions<sup>6,7</sup>.

Urban overheating has a serious impact on humans<sup>8</sup>. It increases both the cooling energy consumption of buildings and the peak

electricity demand (obliging utilities to build additional power plants), decreases human productivity, increases the concentration of ground ozone, and leads to surges in heat-related mortality and morbidity while also intensifying human aggressivity and mental health problems<sup>8</sup> (Supplementary Information section 1).

Projections about future urban climatic conditions have shown that minimum and maximum temperatures may increase substantially<sup>9</sup>. The projected increase in the minimum night-time temperature could be as high as 4.0 °C (refs. 10,11), and this will be combined with an increase in exposure to heat waves and ground-level ozone<sup>12,13</sup>. As a result, buildings' energy consumption for cooling may increase by

<sup>1</sup>School of Built Environment, Faculty of Arts, Design and Architecture, University of New South Wales, Sydney, New South Wales, Australia. <sup>2</sup>Building Technology and Urban Systems Division, Lawrence Berkeley National Laboratory, Berkeley, CA, USA. <sup>3</sup>Royal Commission of Riyadh City, Riyadh, Saudi Arabia. <sup>4</sup>Department of Geography, Lalbaba College, University of Calcutta, Kolkata, India. <sup>5</sup>Department of Environmental Physics, National and Kapodistrian University of Athens, Athens, Greece. <sup>6</sup>Anita Lawrence Chair in High Performance Architecture, University of New South Wales, Sydney, New South Wales, Australia. <sup>7</sup>Present address: School of Architecture, Design and Planning, University of Sydney, Sydney, New South Wales, Australia. <sup>8</sup>Present address: Institute of Future Cities, The Chinese University of Hong Kong, Shatin, Hong Kong.  e-mail: [m.santamouris@unsw.edu.au](mailto:m.santamouris@unsw.edu.au)

**Table 1 | Description of the mitigation scenarios**

| No. | Mitigation scenario   | Description   |
|-----|---|---|
| 1   | Reference   | Reference Riyadh: climatic evaluation of the whole Riyadh area for three summer months and one winter month under the existing conditions without application of mitigation measures (albedo of roofs and pavements, 0.20).   |
| 2   | Use of high-albedo material   | Reflective Riyadh: modified high albedo in the whole city of Riyadh using reflective materials. Roofs and pavements with higher albedo than the base case is considered for the whole urban area of Riyadh (albedo of roofs, 0.75; albedo of pavements, 0.40).  |
| 3   | Use of super-cool material  | Very Reflective Riyadh: modified very high albedo in the whole city of Riyadh. City-wide implementation of super-cool materials (photonic daytime radiative coolers), in roofs with an albedo of 0.95 and emissivity in the atmospheric window of 0.95. No modification of the albedo of pavements, as under the current conditions.  |
| 4   | 30% low-level non-irrigated vegetation cover  | Green and Dry Riyadh: increase of the green infrastructure of Riyadh of up to 30% of its surface using non-irrigated low-level vegetation (shrubs and grass). Albedo as under the current conditions.   |
| 5   | 60% low-level non-irrigated vegetation cover  | Very Green and Dry Riyadh: increase of the green infrastructure of Riyadh up to 60% of its surface, using non-irrigated low-level vegetation (shrubs and grass). Albedo as under the current conditions.  |
| 6   | 30% low-level irrigated vegetation cover  | Green and Irrigated Riyadh: increase of the green infrastructure of Riyadh up to 30% of its surface, using irrigated low-level vegetation (shrubs and grass). Albedo as under the current conditions.   |
| 7   | 60% high-level irrigated vegetation cover   | Very Green and Irrigated Riyadh: increase of the green infrastructure of Riyadh up to 60% of its surface, using irrigated high-level vegetation (broadleaf trees). Albedo as under the current conditions.  |
| 8   | Combination of 60% low-level non-irrigated vegetation cover and super-cool material | Very Green–Very Reflective and Dry Riyadh: combined case—increase of the green infrastructure of Riyadh up to 60% of its surface, using non-irrigated low-level vegetation (shrubs and grass) combined with city-wide implementation of super-cool materials in roofs with an albedo of 0.95 and emissivity of 0.95. No modification of the albedo of pavements, as under the current conditions.   |
| 9   | Combination of 60% high-level irrigated vegetation cover and super-cool material    | Very Green–Very Reflective and Irrigated Riyadh: combined case—increase of the green infrastructure of Riyadh up to 60% of its surface, using irrigated high-level vegetation (broadleaf trees) combined with city-wide implementation of super-cool materials in roofs with an albedo of 0.95 and emissivity of 0.95. No modification of the albedo of pavements, as under the current conditions. |

250–1,000%, with the range depending on global economic and technological developments<sup>14</sup>.

To counterbalance the impact of urban overheating, efficient heat mitigation technologies must be implemented at the city scale. Heat mitigation research has led to innovative technologies that substantially decrease urban temperatures<sup>15</sup>. It is reasonably expected that the development of photonic daytime radiative cooling materials for buildings and urban structures, combined with optimized greenery solutions, will greatly mitigate urban heat<sup>16–18</sup>.

As buildings are responsible for about one-third of global energy consumption, improving building energy efficiency offers a great opportunity to make cities more sustainable environments<sup>19</sup>. It is thus important to investigate strategies to reduce energy use and the corresponding environmental impacts.

Very little is known about the contribution of innovative heat mitigation technologies to the climate of cities and to the related energy-saving potential. Studies assessing the cooling potential of conventional reflecting materials show that it is rational to achieve a drop in peak ambient temperature of up to 1.5 °C and a decrease in the cooling energy demand of 15–35%, depending on the climatic characteristics and quality of the building stock<sup>20,21</sup>. Given the limited number of existing large-scale heat mitigation projects and the absence of detailed assessment studies, there remains a serious lack of knowledge about the exact climatic contributions and energy impact of innovative heat mitigation technologies and the potential of their combined implementation.

This Article presents the methodology, characteristics and results of the largest (to our knowledge) world urban heat mitigation project, designed for the city of Riyadh in Saudi Arabia. We provide innovative information on (1) the assessed climatic capacity of the developed innovative heat mitigation technologies and the combination thereof and (2) their energy potential at the city scale, evaluated for a very high number (3,323) of urban buildings.

We also delve into the compelling relationship between urban heat mitigation and energy conservation, exploring the various strategies

used to counter the rising temperatures in cities and their substantial contributions to promoting energy efficiency, sustainability and urban resilience. Through a comprehensive analysis of the multifaceted impacts of mitigating urban heat, this study sheds light on the pivotal role such measures play in creating more liveable, energy-efficient urban environments. We believe that the Article contributes substantially to the proper design of urban heat mitigation and assesses its energy potential while contributing to the improvement of living conditions, sustainable urban development and urban resilience.

## Results

The distribution of the urban heat risk in the city was assessed using the methodology described in the Methods. Detailed analysis of the current climatic and heat risk conditions in Riyadh, described in the Methods, reveals that the main axes of the potential interventions to mitigate urban heat in Riyadh should aim to (1) decrease the surface, land surface (LST) and ambient temperatures and reduce heat advection from the surrounding desert, (2) reduce the strength of the sensible heat in the city, (3) surge the magnitude of latent heat and (4) improve solar control in the city<sup>22</sup>.

We designed and evaluated eight mitigation scenarios (Table 1) focusing on the above objectives. To decrease the surface temperature in the city and reduce the release of sensible heat, reflective materials and passive daytime radiative cooling coatings were considered. Reflective materials that have a high solar reflectance and a high broadband emittance are commercially available, and can contribute to reducing the LST by up to 10.0 °C (ref. 23). Super-cool materials (SCMs)—or photonic daytime radiative cooling coatings—have been developed recently. Super-cool coatings exhibit sub-ambient surface temperatures and, depending on the local climatic conditions, can reduce the surface temperature of cities by up to 15.0 °C (ref. 16). By lowering the urban surface temperature, the height of the planetary boundary layer may decrease, resulting in reduced heat advection from the desert<sup>24</sup>.

An increase in the green infrastructure in cities provides solar control and decreases the release of sensible heat, while enhancing

**Table 2 | Simulated performance of the eight mitigation scenarios during the summer period, as compared to the reference scenario**

| Scenario   | Reflective Riyadh | Very Reflective Riyadh | Green and Dry Riyadh | Green and Irrigated Riyadh | Very Green Non-Irrigated Riyadh | Very Green and Irrigated Riyadh | Very Green–Very Reflective and Dry Riyadh | Very Green–Very Reflective and Irrigated Riyadh |
|--|-------------------|------------------------|----------------------|----------------------------|---------------------------------|---------------------------------|---|---|
| Decrease maximum summer ambient temperature at 14:00             | 2.2               | 2.3                    | 1.3                  | 1.3                        | 0.8                             | 2.1                             | 1.6                                       | 3.0   |
| Decrease of the mean summer ambient temperature at 14:00         | 1.2               | 1.3                    | −0.1                 | 0.3                        | −0.3                            | 0.6                             | 0.5                                       | 1.4   |
| Decrease of the minimum summer ambient temperature at 14:00      | 0.2               | 0.3                    | −1.5                 | −0.7                       | −1.4                            | −0.9                            | −0.6                                      | 0.0   |
| Decrease of the maximum summer ambient temperature at 06:00      | 3.4               | 3.7                    | 3.3                  | 3.7                        | 5.1                             | 7.0                             | 7.4                                       | 8.6   |
| Decrease of the mean summer ambient temperature at 06:00         | 1.2               | 1.4                    | 0.3                  | 1.1                        | 0.9                             | 2.1                             | 2.1                                       | 3   |
| Decrease of the minimum summer ambient temperature at 06:00      | 1.1               | −0.9                   | −2.8                 | −1.5                       | −3.7                            | −2.8                            | −3.6                                      | −2.8  |
| Decrease of the maximum 24-h summer ambient temperature          | 1.9               | 2.0                    | 4.0                  | 2.6                        | 8.0                             | 7.2                             | 8.5                                       | 7.5   |
| Decrease of the mean 24-h summer ambient Temperature             | 0.9               | 0.9                    | 0.7                  | 1.2                        | 2.3                             | 3.5                             | 2.9                                       | 4.2   |
| Decrease of the 24-h minimum summer ambient temperature at 06:00 | −0.6              | −0.6                   | −2.9                 | 0.2                        | −1.1                            | 0.4                             | −0.3                                      | 1.3   |
| Decrease of the maximum summer surface temperature at 14:00      | 6.2               | 6.6                    | 1.6                  | 4.6                        | 1.7                             | 4.6                             | 5.0                                       | 7.3   |
| Decrease of the mean summer surface temperature at 14:00         | 4.8               | 5.2                    | −0.4                 | 2.0                        | −0.8                            | 2.3                             | 2.6                                       | 4   |
| Decrease of the minimum summer surface temperature at 14:00      | 3.5               | 3.7                    | −2.5                 | 0.1                        | −3.3                            | 0.1                             | 0.2                                       | 3.5   |

latent heat through evapotranspiration<sup>18</sup>. The cooling efficacy of urban greenery under high ambient temperatures, as in Riyadh, depends highly on the proper provision of irrigation<sup>25</sup>. Above a threshold ambient temperature and under low watering conditions, the magnitude of evapotranspiration is reduced significantly, while the released biogenic volatile compounds (BVOCs), may surge, resulting in serious air-quality problems<sup>26</sup>.

Combined scenarios considering the implementation of reflective or super-cool materials with additional irrigated or non-irrigated greenery were designed and evaluated through mesoscale climatic modeling. Table 2 provides the calculated cooling performance and the corresponding mitigation potential for the ambient and surface temperatures for the eight scenarios. Supplementary Table 4 provides the calculated mean, maximum and minimum average values of the main climatic parameters for the reference and eight mitigation scenarios, and Supplementary Table 5 presents the number of hours that the average temperature in Riyadh is above a threshold as well as the corresponding value of the cooling degree hours (CDHs) during the whole summer period.

Analysis of the performance of the eight mitigation scenarios leads to the following main findings:

- An almost linear association between the reference temperature (no mitigation) and the potential temperature decrease is observed for both day and night periods. This is because mitigation technologies decrease the released sensible heat, which is almost a linear function of the ambient temperature. In general, and for all the mitigation scenarios, the higher the background temperature, the higher the potential temperature decrease. Supplementary Fig. 21 demonstrates the relation of the background temperature with the temperature drop for both day and night and for the scenario Very Reflective Riyadh.
- The implementation of the super-cool materials on the roofs of buildings, combined with well-irrigated additional greenery, provides exceptional mitigation potential and contributes to a reduction of the average 24-h ambient urban temperature of 1.3–7.5 °C, with an average close to 4.2 °C. The corresponding decrease in the ambient temperature at 14:00 varies between 0.0 and 3.0 °C, with

an average close to 1.4 °C, while at 06:00, the change in ambient temperature varies between an increase of 2.8 °C and a decrease of 8.6 °C, with an average close to 3 °C. The reduction in the surface temperature in the city at 14:00 varies between 3.5 and 7.3 °C, with an average close to 4 °C. During the whole summer period, the decrease in the overheating hours above 35 °C and 40 °C is 23.1% and 29.4%, respectively, and the decrease in CDHs with bases of 35 °C and 40 °C is 28.4% and 47.6%, respectively.

- A moderate increase of low-level non-irrigated greenery at the city scale has a limited cooling capacity during daytime, and it may even slightly increase the temperature. This is because the moisture in the top layer of soil decreases due to a lack of precipitation. By increasing the vegetation cover, the moisture level continues to decrease because of the larger surface of evapotranspiration. Under such soil moisture conditions, low-level vegetation with shallow roots can no longer evaporate effectively and plants cannot release latent heat, resulting in a very limited decrease or even increase of the daytime ambient temperature. Similar results were reported in ref. 27 for Los Angeles, where it was demonstrated that replacing existing plants with drought-tolerant plants without irrigation prevents plants from relieving urban heat island (UHI) and heatwave conditions. During the night, the cooling contribution of low-level non-irrigated greenery is more significant, as plants reduce the upward heat flux from the ground, resulting in a cooler soil surface. The average night-time temperature decrease may reach 3.0 °C, in full agreement with many similar studies reporting the cooling potential of greenery in cities<sup>28</sup>.
- A significant increase in the cooling potential of urban greenery is observed when high-level irrigated trees are considered. The average ambient 24-h temperature is found to decrease by between 0.4 °C and 7.2 °C with an average close to 3.5 °C. The average decreases in ambient temperature at 14:00 and 06:00 are 0.6 °C and 2.1 °C, respectively. The overheating hours above 35.0 °C and 40.0 °C decrease by up to 19.1% and 14.1%, respectively, and the decreases in CDHs are 17.1% and 21.5%, respectively.
- Although non-irrigated vegetation shows a cooling effect at night, it is not effective in reducing CDHs during the daytime. Non-irrigated vegetation leads to slightly higher CDHs at a base of 38 °C compared to the reference scenario, and irrigated vegetation reduces CDHs during the day. Shading and evapotranspiration contribute most to the cooling effect of vegetation. The denser the plant canopy, the higher the cooling potential, as long as the plants are sufficiently supplied with water. The cooling potential of trees and other vegetation is severely reduced under dry conditions when soil water is limited, which results in drought stress to the plants and lower evapotranspiration. The variation in CDHs during the day and night for different base temperatures is shown in Supplementary Fig. 22.
- An increase in the urban albedo decreases the peak daytime ambient temperature by between 0.2 and 2.2 °C, with an average close to 1.2 °C, while the corresponding decrease of the LST is 4.8 °C. Reflecting materials decrease the CDHs for base temperatures of 35.0 °C and 40.0 °C by 19.5% and 47.6%, respectively, while the corresponding decreases in overheating hours are 7.0% and 24.1%.
- Implementation of passive daytime radiative cooling materials on the roofs of buildings presents a very significant heat mitigation potential, because the high reflectance and high emissivity in the atmospheric window decrease the peak ambient temperature at 14:00 by between 0.3 °C and 2.3 °C with an average of 1.3 °C, and the LST by 6.6 °C. Super-cool materials contribute to the decrease in CDHs for base temperatures of 35.0 °C and 40.0 °C by 21.9% and 50.8%, respectively, with corresponding decreases in overheating hours of 8% and 28.1%. Given the very high reflectance of super-cool materials, their use should be limited on roofs to avoid optical annoyance issues.

Using the CityBES simulation platform, the cooling energy consumption of 3,323 buildings located in the Al Masiaf precinct of Riyadh was evaluated for the entire summer period, using weather files corresponding to current climatic conditions as well as to the eight designed mitigation scenarios (Fig. 1).

The average summertime cooling load of all the buildings, COP = 1, is 104.6 kWh m<sup>-2</sup>, and the total summertime cooling load of all the buildings is 222.3 GWh. As expected, the taller the building, the lower the cooling load. The average loads for one-, two-, three- and four-storey buildings are 122.1 kWh m<sup>-2</sup>, 103.3 kWh m<sup>-2</sup>, 103 kWh m<sup>-2</sup> and 88.2 kWh m<sup>-2</sup>, respectively (Fig. 2).

The calculated average summertime cooling loads corresponding to the eight mitigation scenarios are given in Table 3. Calculations for all cases were performed using the same building characteristics considered in the reference scenario (Supplementary Table 1). The albedo of the buildings was not modified, so as to assess the cooling contribution caused by the temperature reduction induced by the mitigation technologies and not because of the reduced solar absorption by the structure of the building.

As shown, the mitigation scenarios investigated here result in a decrease in the average summertime cooling that ranges from 3.6% to 16%. The use of high-albedo and super-cool materials reduces the cooling load by 4.4% and 5.2%, respectively, compared to the reference scenario. The Green and Dry and Very Green and Dry scenarios lead to decreases of 3.9% and 10.6% of the average cooling loads compared to the reference, but this reduction is slightly higher when considering irrigated vegetation (5.4% and 13.4%, respectively). The combination of Very Reflective and Very Green with a non-irrigated vegetation scenario shows a 14.8% reduction in the average cooling loads. The maximum reduction (16.0%) in the average cooling load is achieved by the combination of Very Reflective and Very Green with the irrigated vegetation scenario. Residential buildings present a slightly higher decrease in their cooling load than commercial buildings because of the lower internal gains. The implementation of heat mitigation technologies in the considered urban area can provide a reduction of the cooling load of up to 35.5 GWh during the summer period. Extended Data Fig. 1 demonstrates the distribution of the annual cooling load in the study area for the eight investigated mitigation scenarios.

The energy conservation potential of building envelope-related mitigation technologies increases substantially when a reduction in absorbed solar radiation is considered. Supplementary Table 5 presents the cooling load reductions in buildings of one to four storeys under reflective and very reflective mitigation scenarios, considering both direct and indirect benefits arising from the implementation of reflective and super-cool materials on roofs. Under the reflective scenario, when considering the decrease in absorbed solar radiation, the cooling load conservation increases on average from 4.4% to 5.6%. Under the very reflective scenario, the cooling load conservation increases from 5.2% to 6.9%. In absolute values, the total cooling load reduction in the urban area under the reflective scenario will rise from 9.8 GWh to 12.4 GWh, and for the very reflective scenario the corresponding reductions are 11.6 GWh and 15.3 GWh. The calculated reductions indicate that, in both scenarios, almost 75–78% of the potential conservation of the cooling load in the 3,323 buildings is attributed to the decrease in ambient temperature induced by implementation of the mitigation technologies underlying the energy conservation impact and the considerable decarbonization potential of urban heat mitigation technologies.

Energy retrofitting of buildings is the most efficient way to decrease their energy demand. To evaluate the combined impact of energy retrofitting and heat mitigation technologies implemented at the building and city scales, we designed and simulated the energy impact of retrofitting measures for all 3,323 buildings, combined with heat mitigation technologies implemented at the urban scale. Energy retrofitting included measures to improve the thermal quality of the

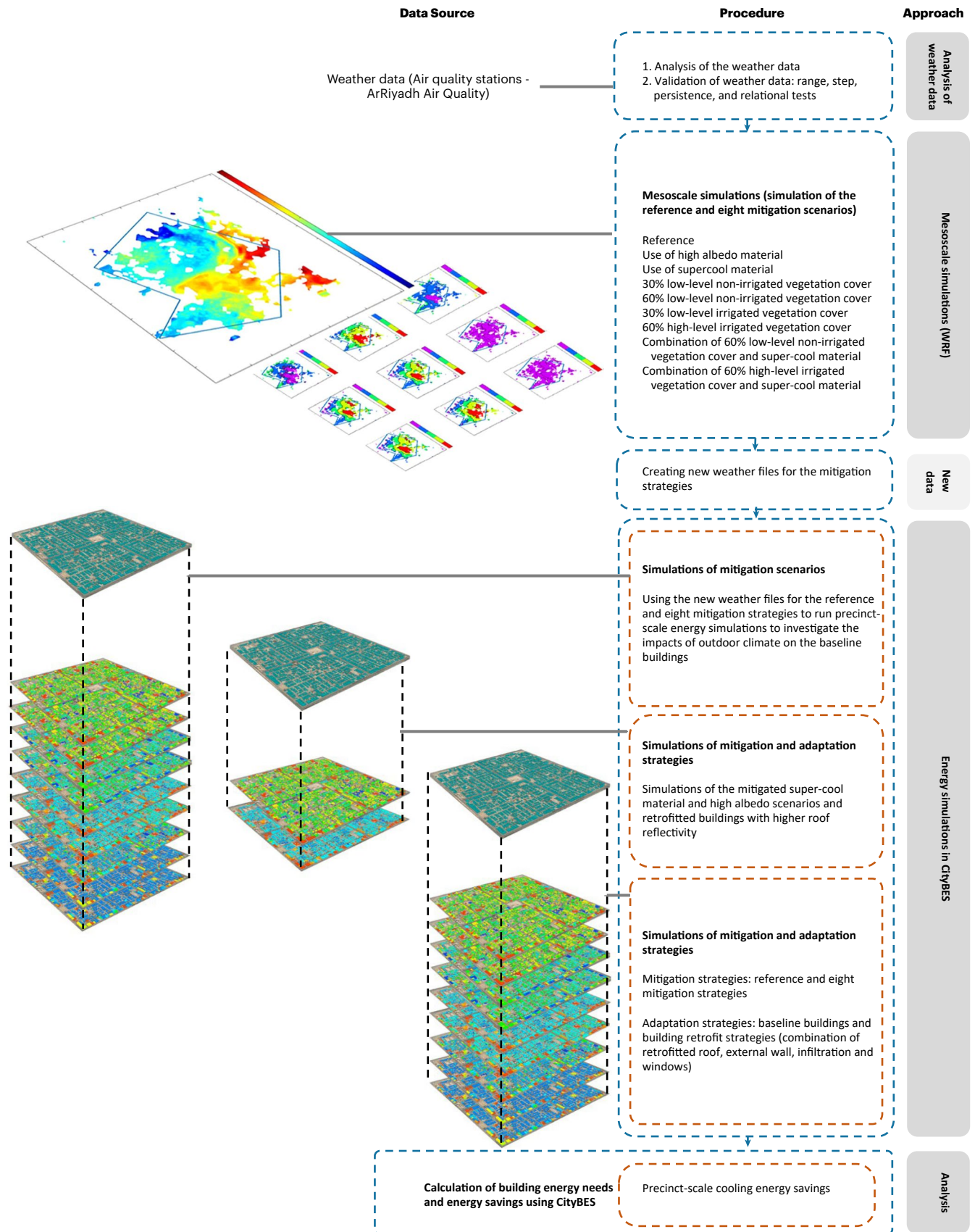


**Fig. 1 | The methodology followed.** The main methodological approaches and framework used in this study are presented.





**Fig. 2 | Cooling load of the buildings.** Distribution of the calculated annual cooling load of the buildings under reference conditions.

**Table 3 | Average summer cooling load of all the buildings, as well as the cooling energy conservation percentage under the reference and eight considered mitigation scenarios**

| Scenario  | Reference Riyadh | Reflective Riyadh | Very Reflective Riyadh | Green and Dry Riyadh | Green and Irrigated Riyadh | Very Green Non-Irrigated Riyadh | Very Green and Irrigated Riyadh | Very Green–Very Reflective and Dry Riyadh | Very Green–Very Reflective and Irrigated Riyadh |
|---|------------------|-------------------|------------------------|----------------------|----------------------------|---------------------------------|---------------------------------|---|---|
| Average summer cooling load, (kWhm <sup>-2</sup> )      | 104.6            | 100.0             | 99.2                   | 100.5                | 98.9                       | 93.5                            | 90.6                            | 89.1                                      | 87.9  |
| Reduction of the cooling load against the reference (%) | –                | 4.4               | 5.2                    | 3.9                  | 5.4                        | 10.6                            | 13.4                            | 14.8                                      | 16.0  |

envelope, namely better windows, better insulation, improved solar control, cool roofs and improved air permeability. Measures related to heating, ventilation and air-conditioning (HVAC) systems were not considered. A list of the selected energy retrofitting measures is provided in Supplementary Table 6.

The calculated reductions in the summer cooling load in the urban area, considering a combined implementation of heat mitigation and energy retrofitting measures ( $Q_{comb}$ ) and also the corresponding cooling benefits ( $Q_{mit}$ ) when only mitigation measures are considered, are provided in Extended Data Table 1. Because of the important thermal interaction between the energy retrofitting and heat mitigation measures during building operations, the difference  $Q_{comb} - Q_{mit}$  does not represent the exact contribution of the retrofitting measures and is lower than when retrofitting measures are applied individually. Simulation of the energy impact of the retrofitting measures under non-mitigated climatic conditions was also performed for all the buildings, and the corresponding reduction in the cooling load of the reference building was calculated ( $Q_{retr}$ ). However, under combined implementation of the mitigation and retrofitting measures, the real contributions of the heat mitigation and energy retrofitting measures

are lower than  $Q_{mit}$  and  $Q_{retr}$ , respectively, because of the important thermal interaction between the considered measures. Nevertheless, a comparison between  $Q_{mit}$  versus  $Q_{comb}$  and  $Q_{retr}$  versus  $Q_{comb}$  can provide an approximate but quite realistic contribution of the mitigation and retrofitting technologies. As shown in Extended Data Table 1, combined heat mitigation technologies can contribute up to 46% of the total cooling load conservation of urban buildings under the combined implementation of heat mitigation and energy retrofitting measures.

To assess the heat risk for Riyadh, several climatic, demographic and socioeconomic parameters were combined into a composite heat risk indicator, as described in the Methods. It was found that the north-east and southeast districts of the city (in red) have higher heat risk than those to the west of the city. Several districts in the center of the city also exhibit high thermal risk (Fig. 3).

### Discussion

The temperature of cities is steadily increasing, and is expected to increase further as a result of intensive urbanization, overpopulation and global climate change<sup>10</sup>. To lower urban air and surface temperatures and counterbalance the impact of high temperatures on the

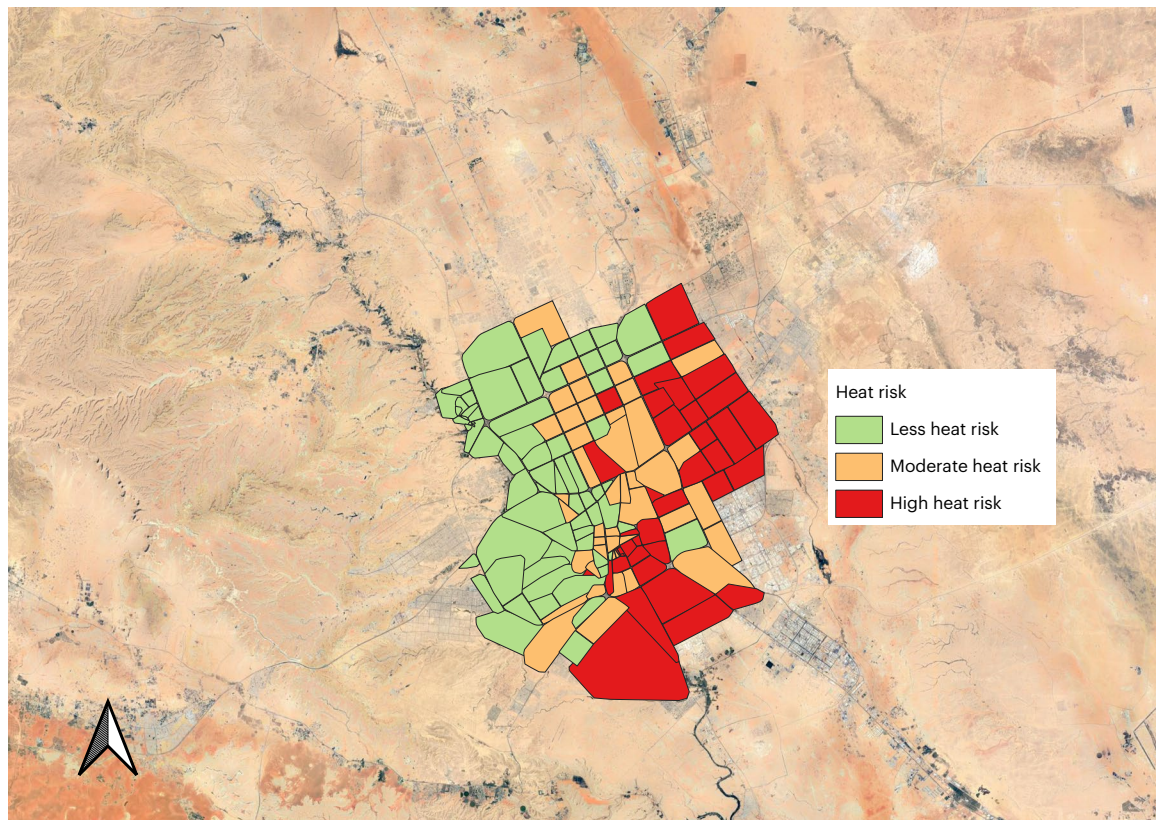


**Fig. 3 | Distribution of heat indicator.** Spatial distribution of the value of the composite heat indicator in Riyadh.

energy demand for cooling, heat mitigation technologies have been developed and implemented. Although the impact of conventional mitigation technologies has been assessed for several cities, there are important knowledge gaps regarding the mitigation potential of innovative technologies such as daytime radiative cooling materials, the specific impact of irrigated or non-irrigated greenery, and the combined effects of materials and greenery on the energy impact of heat mitigation at the urban scale.

This Article presents a study investigating the large-scale energy benefits of advanced and conventional single and combined heat mitigation technologies implemented at the city scale. The results shown here provide the data necessary to mitigate urban heat and reduce energy use in urban settlements based on interactions between urban building energy demand and the urban climate.

Increasing the urban green infrastructure is the most commonly considered mitigation technology. We show that the main driver for cooling is to improve the transpiration efficiency of plants so that they can reduce the released sensible heat and increase the flux of latent heat flow. Transpiration can normally evaporate water at a rate of  $0.28\text{--}12\text{ l m}^{-2}$  per day<sup>29</sup>, generating a cooling power ranging between  $24.5$  and  $29.5\text{ MJ m}^{-2}$  per day in arid environments with sufficient water supply. However, this is less than  $10\text{ MJ m}^{-2}$  in a temperate climate<sup>26</sup>. The results from the irrigated scenarios show that irrigation is a key factor in achieving an appreciable mitigation effect for vegetation-based mitigation strategies in Riyadh and other hot arid cities. The daytime transpiration of both low-rise vegetation and high-rise vegetation is strongly enhanced by introducing irrigation<sup>30</sup>. In the absence of irrigation, evapotranspiration cannot be effectively stimulated. Furthermore, the dry soil conditions prevent plants from effective evapotranspiration during the day, and most of the contribution to the latent heat flux during the day comes from direct soil evapotranspiration.

Irrigated greenery presents a considerable mitigation potential, especially during the night. On average, irrigated greenery in the city

may decrease the peak day-time temperature by up to  $0.7\text{ }^{\circ}\text{C}$  and the night temperature by up to  $2.1\text{ }^{\circ}\text{C}$ . This agrees with similar studies reported in refs. 28,29,31.

High urban temperatures affect the physiological processes of greenery and their transpiration capacity, resulting in a much lower cooling potential and inappropriate environmental quality<sup>32</sup> (Supplementary Information section 2). Experiments have shown that well-irrigated plants maintain their sap flow during heat waves, but in non-irrigated plants the sap flow is reduced by 50% (ref. 33). Future research should aim to develop more heat-tolerant species, as genetic engineering of plants has progressed to the point where genes with the proper traits can be introduced and expressed efficiently<sup>34</sup>.

Although numerous publications have investigated the impact of urban greenery on representative buildings, very few studies have assessed the benefits at the city or neighborhood levels<sup>35–38</sup>. In addition, although existing articles reflect high non-homogeneity regarding the considered urban climate, the levels of urban overheating, the type of greenery, quality of buildings and assessment methodology, important conclusions can be drawn:

- The 24-h average temperature decrease induced by additional urban greenery varies between  $0.2$  and  $2.5\text{ }^{\circ}\text{C}$ . Most articles report an average 24-h temperature drop of between  $0.7\text{ }^{\circ}\text{C}$  and  $2.2\text{ }^{\circ}\text{C}$ , without specifying the irrigation status. In this study, a moderate rise in urban greenery (30%) decreases the 24-h ambient temperature by between  $0.7\text{ }^{\circ}\text{C}$  (non-irrigated) and  $1.2\text{ }^{\circ}\text{C}$  (irrigated), and a high increase in green infrastructure (60%) results in a temperature decrease of between  $2.3\text{ }^{\circ}\text{C}$  and  $3.5\text{ }^{\circ}\text{C}$ .
- Previous studies agree that most of the cooling benefits from urban greenery occur during the night, and the temperature decrease during the peak daytime period is between  $0.0\text{ }^{\circ}\text{C}$  and  $1.0\text{ }^{\circ}\text{C}$ , with an average close to  $0.4\text{ }^{\circ}\text{C}$ . Almost all studies have been performed for temperate climates and non-arid urban zones,

except ref. 27, which reported a relative increase in the ambient temperature when non-irrigated plants were considered. Similar results were obtained in the present study for non-irrigated plants, and the peak temperature decrease varied between 0.3 °C and 0.6 °C when irrigation was considered.

- The potential decrease in cooling load induced by urban greenery is reported by very few publications. A direct comparison is almost impossible given the different climatic conditions, building stock and characteristics of the greenery. Annual cooling energy conservations varying between 2 and 14 kWh m<sup>-2</sup> are reported, close to the results of the present study for non-irrigated greenery (4 kWh m<sup>-2</sup> and 11 kWh m<sup>-2</sup>), and 5.7 kWh m<sup>-2</sup> to 14 kWh m<sup>-2</sup> for irrigated greenery.

Increasing urban albedo contributes to a decrease in absorbed solar radiation and reduces the urban surface temperature and the release of sensible heat. Previous studies evaluating the impact of modified urban albedo reported a decrease in the 24-h ambient temperature ranging between 0.1 °C and 0.8 °C, and a peak daily temperature reduction of between 0.5 °C and 3.5 °C, depending on the characteristics of the cities and the implemented albedo scenario<sup>39</sup>. It was found that an increase in the albedo by 0.1 results in a decrease in the ambient temperature close to 0.18 °C (at 17:00)<sup>39</sup>. The present study found that the average 24-h and peak daily temperature decreases are 0.9 °C and 1.2 °C, respectively, in full agreement with previous findings.

The recently developed daytime radiative cooling materials have not yet been implemented to mitigate urban overheating. Mesoscale simulations for the city of Kolkata in India have shown that they may decrease the peak urban temperature by up to 4.5 °C, imposing, however, a heating penalty during the winter<sup>40</sup>. Modulation of their optical properties, reflectance and emittance could minimize the problem<sup>41,42</sup>. Simulations have shown that optically modulated super-cool materials can maintain their summer cooling capacity while contributing to increasing the winter ambient temperature by up to 1.5 °C (ref. 43). The present study has found that the average 24-h and peak daily temperature decreases are close to 0.9 °C and 1.3 °C, respectively. The specific values are lower than those reported in ref. 43 as the implementation of the super-cool materials is considered only for roofs. The development of new-generation, colored super-cool materials presenting a lower solar reflectance, but a similar cooling potential, based on the use of fluorescent nanostructures seems to be a major future priority<sup>44</sup>.

Although important recent advances have been achieved in heat mitigation research, significant challenges remain, and future studies need to be developed focusing on a warming climate, mitigation and adaptation technologies, and building energy consumption. The multifaceted strategies employed to mitigate the adverse impacts of UHIs can not only alleviate the discomfort caused by excessive heat, but can also contribute substantially to the broader goals of sustainable urban development and reduced energy consumption.

The findings emphasize the effectiveness of various urban heat mitigation techniques in curbing energy usage, and can be used to design and implement heat mitigation techniques in other cities. The proposed methodology as well as the obtained results and generated knowledge can be implemented elsewhere to improve the performance of the considered heat mitigation techniques, lower electricity consumption and reduce carbon emissions, thus contributing to the overall sustainability of cities.

## Methods

We have designed a research methodology that includes three main tasks. First, a detailed mesoscale simulation of the climatic conditions in the city is performed and validated against extensive existing climatic data. Model results validation is a critical step that underpins the credibility and utility of modeling efforts. It transforms models from theoretical constructs to practical tools that can inform, guide

and drive meaningful real-world outcomes. Further to its validation, the mesoscale model was used to populate the climate data of Riyadh at improved spatial resolution to obtain a more complete view of spatial and temporal trends and differentiations. In the second stage, based on analysis of the climatic conditions, eight heat mitigation strategies and corresponding scenarios were designed and evaluated in terms of their performance using mesoscale climatic modeling. Finally, detailed precinct-scale cooling energy simulations were performed for the Al Masi'af central area, including 3,323 urban buildings.

Climatic simulations were performed using the Weather Research and Forecasting (WRF) model, version 4.2.1<sup>45</sup>. The simulation domain was centered on the city of Riyadh, and three one-way nested domains with horizontal resolutions of 4.5 km, 1.5 km and 0.5 km were used, where the innermost domain was Riyadh city. The outer two domains were used to provide boundary conditions for the innermost domain (Supplementary Figs. 1 and 2). Supplementary Information section 1 provides detailed information about the implementation of the WRF model. The developed mesoscale model was used to calculate the hourly distribution of the main climatic parameters for the entire summer in the city of Riyadh, under existing conditions and the eight mitigation scenarios. The hourly outputs from the nearest grid close to Al Masi'af precinct were used to create nine weather files for the purpose of energy simulations representing the reference climate conditions and all mitigation scenarios. The results obtained from the reference scenario mesoscale simulation were validated against the observations from three existing weather stations to ensure the performance of the model. Validation was performed for both the summer and winter periods and for the most important climatic parameters: ambient temperature, wind speed and relative humidity. We obtained a satisfactory agreement between the simulated and experimental data. The simulation results slightly overestimated the wind speed, which could result from an underestimation of building heights. Details of the validation exercise are provided in Supplementary Information section 1. Supplementary Figs. 3 and 4 present the simulated and experimental data for the three stations.

Riyadh, the capital of Saudi Arabia, has a hot desert climate, 'Bwh', based on the Köppen–Geiger climate classification system<sup>46</sup>. The magnitude of the UHI in Riyadh is persistent and well-captured by the network of stations. The temperature distribution is rather regular, with almost no outliers, and high daily average temperatures exceeding 40.0 °C. The differences between urban and reference contexts are systematic and stable, with frequent peaks exceeding 4.0 °C and differences nearing 1.8 °C for 75% of the examined period (third quartile) and a median of 1.2 °C (Supplementary Fig. 6b). Negative values, namely when the city is cooler than the surroundings because of the advection of cool air from the surroundings, are rarely computed (Supplementary Fig. 6a). Additional information on the climatic analysis is provided in Supplementary Information section 1.

The cooling degree days (CDDs) in Riyadh are quite consistent over the observed period, with very high values exceeding 2,000 at all locations (Supplementary Fig. 7), excluding stations 1 and 4 (Supplementary Table 2). The CDDs at urban locations are -280 higher than those at reference locations. The five-year average of the CDDs at reference (background non-urban) locations is equal to 1,960, and is 2,236 at urban locations. Within the city, there is a difference of 160 CDDs between the hottest and coolest urban areas. These important intra-urban and urban-reference differences point out the influence of local factors such as land cover and wind patterns<sup>47</sup>.

The analysis performed on the integrated dataset (measured and simulated data) provides the following results/conclusions.

- During the hottest conditions and considering all data points, more than 50% of the air temperature data exceed 40.0 °C, and 10% of the urban area has an air temperature higher than 45.0 °C. In contrast, on an average summer day, only 23% of the urban data points have air temperatures exceeding 40.0 °C, and the air temperature does not exceed 45.0 °C. This result shows that in

the hottest climatic conditions, hot spots are not limited, and a considerable number of urban areas experience high ambient temperatures.

- The average simulated UHI intensity of the entire urban area during the summer period is 1.5 °C (Supplementary Fig. 12). The southern and eastern parts have the highest UHI, with an average intensity of more than 2.0 °C and a highest average value of 2.5 °C. The mean UHI intensity increases with increasing urban density. The mean UHI intensity corresponding to low-density urban cells exceeds 2.0 °C for 6% of the time. In medium-density and high-density areas, the corresponding percentages of time are 24.6% and 36.6%, respectively.
- The maximum calculated daytime UHI intensity in the whole city was close to 8.5 °C and appeared at 14:00 (Supplementary Fig. 13). The southeastern part of the city experienced a high UHI intensity of above 8.0 °C. The maximum UHI intensity occurs during northern winds, and the minimum intensity corresponds to southern and southwest winds.
- LST values in the Riyadh urban zone presents substantial variability. Up to 5.0 °C higher average surface temperatures are observed in the southern and southeastern parts of the city (Supplementary Fig. 10). The LSTs in Riyadh have values higher than 50.0 °C during the summer months in all districts, but districts in the northeast and southeast exhibit LSTs even higher than 58.0 °C. This is an important finding, as the LST drives the transfer of heat from the ground to the overlying air and thus contributes to higher air temperatures and reduces soil humidity. The LST at 14:00 ranges between 46.1 °C and 53.3 °C. Additional data about the distribution of LSTs in the city obtained from Landsat 8 satellite observations at 10:30 local time per district were used to reveal, using QGIS software, the most thermally stressed districts of the city. Supplementary Fig. 14 shows the distribution of the mean daily LST by district during a hot day, as calculated by Landsat 8.

High temperatures in urban areas have a direct impact on human health and are associated with heat-related stress and excess summer deaths<sup>48</sup>. We assessed the distribution of the urban heat risk in the city based on daytime LST (Supplementary Fig. 15), Thom discomfort index (Supplementary Fig. 16), air temperature (Supplementary Fig. 17), the percentage of residents under 14 years old (Supplementary Fig. 18), the percentage of residents over 65 years old (Supplementary Fig. 19) and building density (Supplementary Fig. 20), computed for each district of the city. Districts exhibiting high temperature values and inhabited by a high percentage of elderly people are more vulnerable to extreme heat than districts characterized by lower temperature values and a population consisting of younger people.

To assess the heat risk of Riyadh, the parameters presented above were combined into a composite heat risk indicator. To achieve this, each parameter was reclassified into three categories using quantile classification, a data classification method that distributes a set of values into groups containing an equal number of values. Supplementary Table 3 provides the ranges of values for the three risk categories by parameter<sup>49,50</sup>. The resulting three categories were defined: (1) low heat risk, (2) moderate heat risk and (3) high heat risk. Because the relative importance of each parameter is unknown, all parameters contributed equally to the composite heat risk index. The considered parameters were reclassified into three categories using the quantile classification method, resulting in the composite heat risk index

The 3,323 buildings selected for cooling energy simulations are located in the Al Masi'af precinct, which covers an area of ~2 km × 2 km (Supplementary Fig. 5), with the 3,323 buildings including residential buildings (2,962 multi-family and 98 single-family houses) and office buildings (1 large, 241 small and 21 medium offices). The simulated buildings consist of residential and commercial buildings of one to

four storeys. The total area of the selected buildings simulated is 2,125,820 m<sup>2</sup>.

The simulation platform CityBES<sup>51,52</sup> was used to run the energy simulations for Al Masi'af precinct. CityBES is a web-based data and computing platform developed by Lawrence Berkeley National Laboratory (LBNL) to evaluate the energy performance of city buildings. CityBES is organized into three layers: (1) the data layer, (2) the simulation engine (algorithm) and software tools layer, and (3) the use-cases layer. CityBES<sup>52,53</sup> offers a detailed energy performance analysis built on the EnergyPlus engine for dynamic energy simulation of urban buildings, which offers the highest resolution due to its physics-based modeling approaches capturing the full dynamics of the building performance. Specific information and details about the specific simulation procedure are provided in Supplementary Information section 1. The most common construction and operational characteristics of the residential and commercial buildings in Al Masi'af precinct were identified and then used to perform the building energy simulations. Supplementary Table 1 lists the main inputs used to simulate the residential and commercial buildings.

To analyze the current climatic conditions in the city, data from a network of 16 meteorological stations were used (Supplementary Table 2). The dataset analyzed comprises five recent complete years of hourly averages of data from January 2016 to December 2020, representing the current conditions in the city. A detailed statistical methodology, as described in the Supplementary Information, was used to filter the data and control the quality.

We calculated the magnitude of the UHI in the city by considering the difference between a reference (non-urban) station and an urban station, where the reference data were obtained from the average of four meteorological stations located at all four sides of the city. In this way, a reliable appraisal of the differences between the city and its non-urban surroundings was achieved. The difference was calculated by considering a simple moving average over 7 h (3 h backwards, 3 h forwards, and centered on the hour). This approach eliminated short-term differences due to atmospheric circulation conditions and better captures the general trends over the day, as performed in ref. 8.

The climatic information provided by the ground stations was enriched with additional data regarding the spatial distribution of the main climatic parameters, the hottest spots in the city, and the distribution of the latent and sensible heat fluxes as calculated by mesoscale simulations under the current climatic conditions. The calculated spatial distributions of the ambient and surface temperatures, wind speed, UHI intensity and sensible and latent fluxes are provided in Supplementary Figs. 8–13.

### Main limitations of the research

The input data used for the energy simulation of the 3,323 buildings are drawn from the building codes and regulations of the country, although there are potential differences arising from the actual construction characteristics of the buildings. The statistical data utilized for the development of the comfort index represent the latest available information, although it is acknowledged that changes may have occurred.

### Reporting summary

Further information on research design is available in the Nature Portfolio Reporting Summary linked to this Article.

### Data availability

All available data have been uploaded to <https://datadryad.org/stash/share/vap6510fE3EweIUskC2XC7cN0y7qL55MaUjeEZeZcs> and <https://zenodo.org/records/10090715>.

### References

1. Mitchell, L. E. et al. A multi-city urban atmospheric greenhouse gas measurement data synthesis. *Sci. Data* **9**, 361 (2022).

2. SUP – Summary for Urban Policymakers (IPCC, 2022); <https://supforclimate.com/>
3. Oke, T. R. The energetic basis of the urban heat island. *Q. J. R. Meteorol. Soc.* **108**, 1–24 (1982).
4. Founda, D. & Santamouris, M. Synergies between urban heat island and heat waves in Athens (Greece), during an extremely hot summer (2012). *Sci. Rep.* **7**, 10973 (2017).
5. Doblas-Reyes, F. J. et al. in *Climate Change 2021: The Physical Science Basis. Contribution of Working Group I to the Sixth Assessment Report of the Intergovernmental Panel on Climate Change* (eds Masson-Delmotte, V. et al.) 1363–1512 (Cambridge Univ. Press).
6. Tuholske, C. et al. Global urban population exposure to extreme heat. *Proc. Natl Acad. Sci. USA* **118**, 2024792118 (2021).
7. Santamouris, M. Analyzing the heat island magnitude and characteristics in one hundred Asian and Australian cities and regions. *Sci. Total Environ.* **512**, 582–598 (2015).
8. Santamouris, M. Recent progress on urban overheating and heat island research. Integrated assessment of the energy, environmental, vulnerability and health impact. Synergies with the global climate change. *Energy Build.* **207**, 109482 (2020).
9. Hamdi, R. et al. Assessment of three dynamical urban climate downscaling methods: Brussels’s future urban heat island under an A1B emission scenario. *Int. J. Climatol.* **34**, 978–999 (2014).
10. Zhao, L. et al. Global multi-model projections of local urban climates. *Nat. Clim. Change* **11**, 152–157 (2021).
11. Oleson, K. Contrasts between urban and rural climate in CCSM4 CMIP5 climate change scenarios. *J. Clim.* **25**, 1390–1412 (2012).
12. Wang, Y. et al. Future population exposure to heatwaves in 83 global megacities. *Sci. Total Environ.* **888**, 164142 (2023).
13. Jiang, X. et al. Predicted impacts of climate and land use change on surface ozone in the Houston, Texas, area. *J. Geophys. Res. Atmos.* **113**, D20312 (2008).
14. Santamouris, M. Cooling the buildings—past, present and future. *Energy Build.* **128**, 617–638 (2016).
15. Santamouris, M. & Vasilakopoulou, K. Present and future energy consumption of buildings: challenges and opportunities towards decarbonisation. *e-Prime Adv. Electr. Eng. Electr. Energy* **1**, 100002 (2021).
16. Feng, J. et al. The heat mitigation potential and climatic impact of super-cool broadband radiative coolers on a city scale. *Cell Rep. Phys. Sci.* **2**, 100485 (2021).
17. Santamouris, M. & Yun, G. Y. Recent development and research priorities on cool and super cool materials to mitigate urban heat island. *Renew. Energy* **161**, 792–807 (2020).
18. Santamouris, M. et al. Progress in urban greenery mitigation science—assessment methodologies advanced technologies and impact on cities. *J. Civil Eng. Manag.* **24**, 638–671 (2018).
19. Hong, T. et al. Ten questions on urban building energy modeling. *Build. Environ.* **168**, 106508 (2020).
20. Adilkhanova, I., Santamouris, M. & Yun, G. Y. Coupling urban climate modeling and city-scale building energy simulations with the statistical analysis: climate and energy implications of high albedo materials in Seoul. *Energy Build.* **290**, 113092 (2023).
21. Garshasbi, S. et al. On the energy impact of cool roofs in Australia. *Energy Build.* **278**, 112577 (2023).
22. Nazarian, N. et al. Integrated assessment of urban overheating impacts on human life. *Earth’s Future* **10**, 2022EF002682 (2022).
23. Santamouris, M. et al. On the energy impact of urban heat island in Sydney: climate and energy potential of mitigation technologies. *Energy Build.* **166**, 154–164 (2018).
24. Mohamed, A., Khan, A. & Santamouris, M. Numerical evaluation of enhanced green infrastructures for mitigating urban heat in a desert urban setting. *Build. Simul.* **16**, 1691–1712 (2022).
25. Gao, K. & Santamouris, M. The use of water irrigation to mitigate ambient overheating in the built environment: recent progress. *Build. Environ.* **164**, 106346 (2019).
26. Gao, K., Santamouris, M. & Feng, J. On the efficiency of using transpiration cooling to mitigate urban heat. *Climate* **8**, 69 (2020).
27. Vahmani, P. & Ban-Weiss, G. J. G. R. L. Climatic consequences of adopting drought-tolerant vegetation over Los Angeles as a response to California drought. *Geophys. Res. Lett.* **43**, 8240–8249 (2016).
28. Santamouris, M. & Osmond, P. Increasing green infrastructure in cities: impact on ambient temperature, air quality and heat-related mortality and morbidity. *Buildings* **10**, 233 (2020).
29. Nyelele, C., Kroll, C. N. & Nowak, D. J. Present and future ecosystem services of trees in the Bronx, NY. *Urban For. Urban Green.* **42**, 10–20 (2019).
30. Broadbent, A. M. et al. The cooling effect of irrigation on urban microclimate during heatwave conditions. *Urban Clim.* **23**, 309–329 (2018).
31. Duarte, D. H. S. et al. The impact of vegetation on urban microclimate to counterbalance built density in a subtropical changing climate. *Urban Clim.* **14**, 224–239 (2015).
32. Teskey, R. et al. Responses of tree species to heat waves and extreme heat events. *Plant Cell Environ.* **38**, 1699–1712 (2015).
33. Forster, M. & Englefield, A. Can soils assist grapevines in coping with heatwaves? *Soil Sci. Australia* **186**, 16–17 (2018).
34. Harfouche, A., Meilan, R. & Altman, A. Tree genetic engineering and applications to sustainable forestry and biomass production. *Trends Biotechnol.* **29**, 9–17 (2011).
35. Konopacki, S. & Akbari, H. *Energy Savings for Heat-Island Reduction Strategies in Chicago and Houston (Including Updates for Baton Rouge, Sacramento and Salt Lake City)* (UNT Digital Library, 2002).
36. Haddad, S. et al. Integrated assessment of the extreme climatic conditions, thermal performance, vulnerability and well-being in low-income housing in the subtropical climate of Australia. *Energy Build.* **272**, 112349 (2022).
37. Yenneti, K. et al. Urban overheating and cooling potential in Australia: an evidence-based review. *Climate* **8**, 126 (2020).
38. Garshasbi, S. et al. Urban mitigation and building adaptation to minimize the future cooling energy needs. *Sol. Energy* **204**, 708–719 (2020).
39. Santamouris, M. & Fiorito, F. On the impact of modified urban albedo on ambient temperature and heat related mortality. *Sol. Energy* **216**, 493–507 (2021).
40. Khan, A. et al. Optically modulated passive broadband daytime radiative cooling materials can cool cities in summer and heat cities in winter. *Sustainability* **14**, 1114 (2022).
41. Ulpiani, G. et al. On the energy modulation of daytime radiative coolers: a review on infrared emissivity dynamic switch against overcooling. *Sol. Energy* **209**, 278–301 (2020).
42. Tang, K. et al. Temperature-adaptive radiative coating for all-season household thermal regulation. *Science* **374**, 1504–1509 (2021).
43. Khan, A. et al. On the winter overcooling penalty of super cool photonic materials in cities. *Solar Energy Adv.* **1**, 100009 (2021).
44. Jeon, S. et al. Multifunctional daytime radiative cooling devices with simultaneous light-emitting and radiative cooling functional layers. *ACS Appl. Mater. Interfaces* **12**, 54763–54772 (2020).
45. Chen, F. & Dudhia, J. Coupling an advanced land surface-hydrology model with the Penn State-NCAR MM5 modeling system. Part I: model implementation and sensitivity. *Mon. Weather Rev.* **129**, 569–585 (2001).
46. Kottek, M. et al. World map of the Köppen-Geiger climate classification updated. *Meteorol. Z.* **15**, 259–263 (2006).

47. Santamouris, Mat et al. Urban heat island and overheating characteristics in Sydney, Australia. An analysis of multiyear measurements. *Sustainability* **9**, 712 (2017).
48. Ngarambe, J., Santamouris, M. & Yun, G. Y. The impact of urban warming on the mortality of vulnerable populations in Seoul. *Sustainability* **14**, 13452 (2022).
49. Oleson, K. W. et al. Interactions between urbanization, heat stress and climate change. *Clim. Change* **129**, 525–541 (2015).
50. Bhattacharjee, S. et al. Assessment of different methodologies for mapping urban heat vulnerability for Milan, Italy. In *IOP Conference Series: Earth and Environmental Science* **290**, 012162 (IOP Publishing, 2019).
51. Hong, T. et al. CityBES: a web-based platform to support city-scale building energy efficiency. *Urban Comput.* **14**, 2016 (2016).
52. Chen, Y., Hong, T. & Piette, M. A. City-scale building retrofit analysis: a case study using CityBES. In *Proc. Building Simulation 2017: 15th Conference of IBPSA* (eds Barnaby, C. S. & Wetter, M.) 259–266 (IBPSA, 2017).
53. Chen, Y., Hong, T. & Piette, M. A. Automatic generation and simulation of urban building energy models based on city datasets for city-scale building retrofit analysis. *Appl. Energy* **205**, 323–335 (2017).

## Acknowledgements

We gratefully acknowledge the support of the Royal Commission of Riyadh City for their contribution to the project ‘Strategic study on urban heat and mitigation potential in Riyadh—Kingdom of Saudi Arabia Cooling Riyadh’.

## Author contributions

The project was led by M.S., who was responsible for designing the mitigation scenarios and analyzing the data. S.H. coordinated the energy study and analyzed the energy data. W.Z. and T.H. conducted the energy simulations, and K.G. handled the mesoscale simulations. R.P. conducted the local climatic analysis, and C.C. and A.P. focused

on the composite heat risk indicator study and provided remote sensing data. A.K. contributed to the mesoscale simulations. M.A., A.A.M. and A.B. provided essential local data and supervised the study. The manuscript was collectively written by M.S. and S.H., with contributions from all authors.

## Competing interests

The authors declare no competing interests.

## Additional information

**Supplementary information** The online version contains supplementary material available at <https://doi.org/10.1038/s44284-023-00005-5>.

**Correspondence and requests for materials** should be addressed to Mattheos Santamouris.

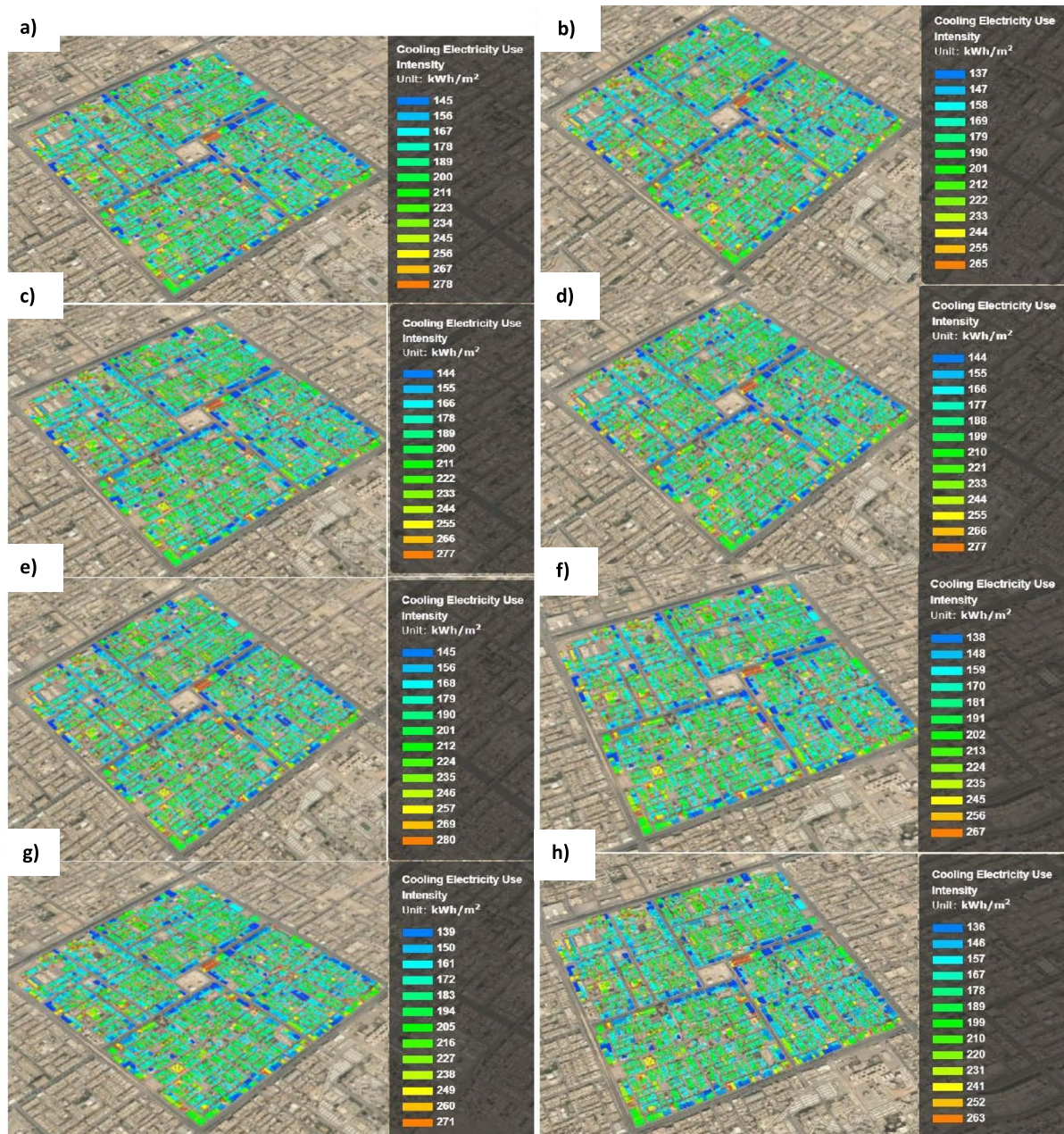
**Peer review information** *Nature Cities* thanks Rafiq Hamdi, M. Abdul Mujeebu, and the other, anonymous, reviewer(s) for their contribution to the peer review of this work.

**Reprints and permissions information** is available at [www.nature.com/reprints](http://www.nature.com/reprints).

**Publisher’s note** Springer Nature remains neutral with regard to jurisdictional claims in published maps and institutional affiliations.

Springer Nature or its licensor (e.g. a society or other partner) holds exclusive rights to this article under a publishing agreement with the author(s) or other rightsholder(s); author self-archiving of the accepted manuscript version of this article is solely governed by the terms of such publishing agreement and applicable law.

© The Author(s), under exclusive licence to Springer Nature America, Inc. 2024



**Extended Data Fig. 1 | The distribution of the annual cooling load of the buildings for the eight mitigation scenarios. a)** Reflective Riyadh, **b)** Very Reflective and Dry Riyadh, **c)** Very Reflective Riyadh, **d)** Green and Irrigated Riyadh, **e)** Green and Dry Riyadh, **f)** Very Green and Irrigated Riyadh, **g)** Very Green and Dry Riyadh, **h)** Very Reflective and Irrigated Riyadh.

**Extended Data Table 1 | Total Reduction of the total summer Cooling Load of the 3323 buildings**

| Scenario  | Reflective Riyadh | Very Reflective Riyadh | Green and Dry Riyadh | Green and Irrigated Riyadh | Very Green Non-Irrigated Riyadh | Very Green and Irrigated Riyadh | Very Green – Very Reflective and Dry Riyadh | Very Green – Very Reflective and Irrigated Riyadh |
|---|-------------------|------------------------|----------------------|----------------------------|---------------------------------|---------------------------------|---|---|
| Combined Cooling Load Reduction, (GWh)  | 60.0              | 57.8                   | 55.6                 | 57.8                       | 68.9                            | 71.2                            | 73.4  | 77.8  |
| Cooling Load Reduction caused by the Heat Mitigation Measures, (GWh)- Non-Combined Simulation           | 9.8               | 11.5                   | 8.7                  | 12.1                       | 23.6                            | 29.8                            | 33.0  | 35.5  |
| Additional Cooling Load Reduction when retrofitting measures are considered, combined simulation, (GWh) | 50.3              | 46.3                   | 46.9                 | 45.7                       | 45.3                            | 41.4                            | 40.4  | 42.3  |
| Potential Percentage Contribution of the Heat Mitigation Measures (%)                                   | 16                | 20                     | 16                   | 21                         | 34                              | 42                              | 45  | 46  |

Calculated under the combined energy retrofitting and heat mitigation simulation and the single heat mitigation simulation settings for the eight mitigation scenarios.



## Reporting Summary

Nature Portfolio wishes to improve the reproducibility of the work that we publish. This form provides structure for consistency and transparency in reporting. For further information on Nature Portfolio policies, see our [Editorial Policies](#) and the [Editorial Policy Checklist](#).

### Statistics

For all statistical analyses, confirm that the following items are present in the figure legend, table legend, main text, or Methods section.

- | n/a                                 | Confirmed  |
|-------------------------------------|--|
| <input type="checkbox"/>            | <input checked="" type="checkbox"/> The exact sample size ( $n$ ) for each experimental group/condition, given as a discrete number and unit of measurement  |
| <input type="checkbox"/>            | <input checked="" type="checkbox"/> A statement on whether measurements were taken from distinct samples or whether the same sample was measured repeatedly  |
| <input type="checkbox"/>            | <input checked="" type="checkbox"/> The statistical test(s) used AND whether they are one- or two-sided<br><i>Only common tests should be described solely by name; describe more complex techniques in the Methods section.</i>   |
| <input checked="" type="checkbox"/> | <input type="checkbox"/> A description of all covariates tested  |
| <input type="checkbox"/>            | <input checked="" type="checkbox"/> A description of any assumptions or corrections, such as tests of normality and adjustment for multiple comparisons  |
| <input type="checkbox"/>            | <input checked="" type="checkbox"/> A full description of the statistical parameters including central tendency (e.g. means) or other basic estimates (e.g. regression coefficient) AND variation (e.g. standard deviation) or associated estimates of uncertainty (e.g. confidence intervals) |
| <input checked="" type="checkbox"/> | <input type="checkbox"/> For null hypothesis testing, the test statistic (e.g. $F$ , $t$ , $r$ ) with confidence intervals, effect sizes, degrees of freedom and $P$ value noted<br><i>Give <math>P</math> values as exact values whenever suitable.</i>                                       |
| <input type="checkbox"/>            | <input checked="" type="checkbox"/> For Bayesian analysis, information on the choice of priors and Markov chain Monte Carlo settings   |
| <input type="checkbox"/>            | <input checked="" type="checkbox"/> For hierarchical and complex designs, identification of the appropriate level for tests and full reporting of outcomes   |
| <input checked="" type="checkbox"/> | <input type="checkbox"/> Estimates of effect sizes (e.g. Cohen's $d$ , Pearson's $r$ ), indicating how they were calculated  |

*Our web collection on [statistics for biologists](#) contains articles on many of the points above.*

### Software and code

Policy information about [availability of computer code](#)

Data collection

Data analysis

For manuscripts utilizing custom algorithms or software that are central to the research but not yet described in published literature, software must be made available to editors and reviewers. We strongly encourage code deposition in a community repository (e.g. GitHub). See the Nature Portfolio [guidelines for submitting code & software](#) for further information.

### Data

Policy information about [availability of data](#)

All manuscripts must include a [data availability statement](#). This statement should provide the following information, where applicable:

- Accession codes, unique identifiers, or web links for publicly available datasets
- A description of any restrictions on data availability
- For clinical datasets or third party data, please ensure that the statement adheres to our [policy](#)

All available data are uploaded in :

- a) <https://datadryad.org/stash/share/vap6510fE3EEweIUskC2XC7cN0y7qL55MaUjeEZeZcs>
- b) <https://doi.org/10.5061/dryad.jsxksn0hb>

## Human research participants

Policy information about [studies involving human research participants and Sex and Gender in Research](#).

|                             |   |
|-----------------------------|---|
| Reporting on sex and gender | <input type="text" value="The research did not involved reserach on human"/>                  |
| Population characteristics  | <input type="text" value="The study did not involve reserach on population characteristics"/> |
| Recruitment                 | <input type="text" value="We have not recruited any participants"/>                           |
| Ethics oversight            | <input type="text" value="Royal Commission of Riyadh"/>                                       |

Note that full information on the approval of the study protocol must also be provided in the manuscript.

## Field-specific reporting

Please select the one below that is the best fit for your research. If you are not sure, read the appropriate sections before making your selection.

Life sciences     Behavioural & social sciences     Ecological, evolutionary & environmental sciences

For a reference copy of the document with all sections, see [nature.com/documents/nr-reporting-summary-flat.pdf](https://www.nature.com/documents/nr-reporting-summary-flat.pdf)

## Ecological, evolutionary & environmental sciences study design

All studies must disclose on these points even when the disclosure is negative.

|                                   |  |
|-----------------------------------|--|
| Study description                 | <input type="text" value="Advanced urban heat mitigation technologies that involve the use of super cool materials combined with properly designed green infrastructure, lower the urban ambient and land surface temperatures and reduce the cooling consumption at the city scale. We present the results of the world's largest heat mitigation project in Riyadh, KSA. Daytime radiative coolers as well as cool materials combined with irrigated or non-irrigated greenery, have been used to design eight holistic heat mitigation scenarios. We assessed the climatic impact of the scenarios as well as the corresponding energy benefits of 3323 urban buildings. An impressive decrease of the peak ambient temperature, up to 4.5°C, is calculated, consisting of the highest reported urban ambient temperature reduction, while the annual sum of the differences of the ambient temperature against a standard temperature base, (cooling degree hours), in the city decrease by up to 26%. We found that innovative urban heat mitigation strategies contribute to remarkable cooling energy conservation by up to 16%, while the combined implementation of heat mitigation and energy adaptation technologies decrease the cooling demand by up to 35%. It is the first article investigating the large-scale energy benefits of modern heat mitigation technologies when are implemented in cities"/> |
| Research sample                   | <input type="text" value="The whole city of Riyadh, Saudi Arabia"/>  |
| Sampling strategy                 | <input type="text" value="The study do not include a samplecollection"/>   |
| Data collection                   | <input type="text" value="WE collected data from all existing meteo stations in Riyadh. We filtered all data cording to the methodology described in the article"/>  |
| Timing and spatial scale          | <input type="text" value="the study is performed for both the summer and winter period"/>  |
| Data exclusions                   | <input type="text" value="We have excluded meteo data that failed to pass the statistical control"/>   |
| Reproducibility                   | <input type="text" value="The study did not involved experiments."/>   |
| Randomization                     | <input type="text" value="The study did not included any randomization ."/>  |
| Blinding                          | <input type="text" value="no blinding processes are used"/>  |
| Did the study involve field work? | <input type="checkbox"/> Yes <input checked="" type="checkbox"/> No  |

## Reporting for specific materials, systems and methods

We require information from authors about some types of materials, experimental systems and methods used in many studies. Here, indicate whether each material, system or method listed is relevant to your study. If you are not sure if a list item applies to your research, read the appropriate section before selecting a response.

## Materials & experimental systems

- | n/a                                 | Included in the study                                  |
|-------------------------------------|--|
| <input checked="" type="checkbox"/> | <input type="checkbox"/> Antibodies                    |
| <input checked="" type="checkbox"/> | <input type="checkbox"/> Eukaryotic cell lines         |
| <input checked="" type="checkbox"/> | <input type="checkbox"/> Palaeontology and archaeology |
| <input checked="" type="checkbox"/> | <input type="checkbox"/> Animals and other organisms   |
| <input checked="" type="checkbox"/> | <input type="checkbox"/> Clinical data                 |
| <input checked="" type="checkbox"/> | <input type="checkbox"/> Dual use research of concern  |

## Methods

- | n/a                                 | Included in the study                           |
|-------------------------------------|---|
| <input checked="" type="checkbox"/> | <input type="checkbox"/> ChIP-seq               |
| <input checked="" type="checkbox"/> | <input type="checkbox"/> Flow cytometry         |
| <input checked="" type="checkbox"/> | <input type="checkbox"/> MRI-based neuroimaging |